

# Thermal effects on quark-gluon mixed condensate $g\langle\bar{q}\sigma_{\mu\nu}G_{\mu\nu}q\rangle$ from lattice QCD

Takumi Doi,\* Noriyoshi Ishii, Makoto Oka, and Hideo Suganuma

*Department of Physics, Tokyo Institute of Technology, Ohokayama 2-12-1, Meguro, Tokyo 152-8551, Japan*

(Received 6 February 2004; published 26 August 2004)

We present the first study of the thermal effects on the quark-gluon mixed condensate  $g\langle\bar{q}\sigma_{\mu\nu}G_{\mu\nu}q\rangle$ , which is another chiral order parameter, in the  $SU(3)_c$  lattice QCD with the Kogut-Susskind fermion at the quenched level. Using the lattices at  $\beta=6.0, 6.1, \text{ and } 6.2$  in high statistics, we calculate  $g\langle\bar{q}\sigma_{\mu\nu}G_{\mu\nu}q\rangle$  as well as  $\langle\bar{q}q\rangle$  in the chiral limit for  $0\leq T\leq 500$  MeV. Except for the sharp decrease of both the condensates around  $T_c\approx 280$  MeV, the thermal effects are found to be weak below  $T_c$ . We also find that the ratio  $m_0^2\equiv g\langle\bar{q}\sigma_{\mu\nu}G_{\mu\nu}q\rangle/\langle\bar{q}q\rangle$  is almost independent of the temperature even in the very vicinity of  $T_c$ . This result indicates nontrivial similarity in the chiral behaviors of the two different condensates.

DOI: 10.1103/PhysRevD.70.034510

PACS number(s): 12.38.Gc, 11.15.Ha

## I. INTRODUCTION

Quantum chromodynamics (QCD) exhibits interesting nonperturbative phenomena such as spontaneous chiral-symmetry breaking and color confinement, which are considered to be related to the nontrivial structure of the QCD vacuum. In order to clarify the mechanism of these phenomena and their relation to the QCD vacuum, extensive studies have been made. In fact, at high temperature, QCD is believed to exhibit phase transitions into the quark-gluon plasma (QGP), where chiral symmetry is restored and the color is deconfined. The QGP phase is considered to have actually been realized in the early Universe, and the ongoing RHIC experiments attempt to produce QGP in the laboratory through relativistic heavy-ion collisions, which motivates further studies of finite temperature QCD.

For the theoretical study of the QCD vacuum structure at finite temperature, the condensates such as  $\langle\bar{q}q\rangle$ ,  $\alpha_s\langle G_{\mu\nu}G_{\mu\nu}\rangle$  and  $g\langle\bar{q}\sigma_{\mu\nu}G_{\mu\nu}q\rangle$  play a relevant role, because they characterize the nontrivial QCD vacuum directly. In fact, at finite temperature, changes of the structure of the QCD vacuum will be represented by the thermal effects on the condensates.

In this paper, we study the thermal effects on the quark-gluon mixed condensate  $g\langle\bar{q}\sigma_{\mu\nu}G_{\mu\nu}q\rangle\equiv g\langle\bar{q}\sigma_{\mu\nu}G_{\mu\nu}^A\frac{1}{2}\lambda^Aq\rangle$  for the following reasons. First of all, we note that the chirality of the quark in the operator  $g\langle\bar{q}\sigma_{\mu\nu}G_{\mu\nu}q\rangle$  flips as

$$g\langle\bar{q}\sigma_{\mu\nu}G_{\mu\nu}q\rangle=g\langle\bar{q}_R(\sigma_{\mu\nu}G_{\mu\nu})q_L\rangle+g\langle\bar{q}_L(\sigma_{\mu\nu}G_{\mu\nu})q_R\rangle. \quad (1)$$

Therefore,  $g\langle\bar{q}\sigma_{\mu\nu}G_{\mu\nu}q\rangle$  plays the role of a chiral order

parameter, which can indicate chiral restoration at finite temperature, as well as the usual quark condensate  $\langle\bar{q}q\rangle$ .

Second, we emphasize that  $g\langle\bar{q}\sigma_{\mu\nu}G_{\mu\nu}q\rangle$  characterizes different aspect of the QCD vacuum from  $\langle\bar{q}q\rangle$ . In particular,  $g\langle\bar{q}\sigma_{\mu\nu}G_{\mu\nu}q\rangle$  reflects the color-octet components of quark-antiquark pairs in the QCD vacuum, while  $\langle\bar{q}q\rangle$  reflects only the color-singlet  $q\bar{q}$  components. The mixed condensate  $g\langle\bar{q}\sigma_{\mu\nu}G_{\mu\nu}q\rangle$  thus represents the direct correlation between color-octet  $q\bar{q}$  pairs and the gluon field strength  $G_{\mu\nu}^A$ , i.e., the color electromagnetic field spontaneously generated in the QCD vacuum [1]. Therefore, the thermal effects on  $g\langle\bar{q}\sigma_{\mu\nu}G_{\mu\nu}q\rangle$  in comparison with that of  $\langle\bar{q}q\rangle$  will give new and important information on chiral restoration of the QCD vacuum at finite temperature.

As the third point, we show how the mixed condensate affects the properties of hadrons. To clarify the physical meaning of the condensates, the QCD sum rule is a useful framework, in which the hadronic properties can be directly connected to the various condensates with the help of the dispersion relation [2]. One of the examples where the mixed condensate plays an important role is the QCD sum rule for baryons [3,4]. In the actual calculation of such sum rules, especially in the decuplet baryons, the contribution from  $g\langle\bar{q}\sigma_{\mu\nu}G_{\mu\nu}q\rangle$  amounts to the same magnitude as the leading contribution from  $\langle\bar{q}q\rangle$ , and the mixed condensate has large effects on the  $N\text{-}\Delta$  splitting [4]. In terms of the chiral properties of baryons, the parity splittings of baryons stem from the chiral-odd condensates such as  $\langle\bar{q}q\rangle$  and  $g\langle\bar{q}\sigma_{\mu\nu}G_{\mu\nu}q\rangle$  [5]. Furthermore, recent study [6] shows that the parameter  $g\langle\bar{s}\sigma_{\mu\nu}G_{\mu\nu}s\rangle/\langle\bar{s}s\rangle$  is a key quantity for the prediction on the parity of the recently discovered pentaquark baryon,  $\Theta^+(1540)$  [7]. The mixed condensate is also important in other sum rules such as light-heavy meson systems [8] and exotic meson systems [9]. In these respects, the evaluation of the thermal effects on  $g\langle\bar{q}\sigma_{\mu\nu}G_{\mu\nu}q\rangle$  is expected to give a useful input in QCD sum rules to investigate hadron phenomenology at finite temperature.

\*Present address: RIKEN BNL Research Center, Brookhaven National Laboratory, Upton, New York 11973, USA. Electronic address: doi@quark.phy.bnl.gov

For the analysis of the thermal effects on the mixed condensate  $g\langle\bar{q}\sigma_{\mu\nu}G_{\mu\nu}q\rangle$ , we use lattice QCD Monte Carlo simulation, which is the direct and nonperturbative calculation from QCD. So far, the mixed condensate at zero temperature has been analyzed phenomenologically in the QCD sum rules [10]. In the lattice QCD, a pioneering work [11] was done long time ago, but the result was rather preliminary because the simulation was done with insufficient statistics using a small and coarse lattice. Recently, new lattice calculations have been developed by our group [12] using the Kogut-Susskind (KS) fermion, and by another group [13] using the domain-wall fermion. At finite temperature, however, there has been no result on  $g\langle\bar{q}\sigma_{\mu\nu}G_{\mu\nu}q\rangle$  except for our early reports [14]. Therefore, we present in this paper the first and intensive results of the thermal effects on  $g\langle\bar{q}\sigma_{\mu\nu}G_{\mu\nu}q\rangle$  as well as  $\langle\bar{q}q\rangle$ , including the analysis near the critical temperature.

This paper is organized as follows. In Sec. II, we explain the formalism to evaluate the condensates. In Sec. III, we present the lattice QCD data, and discuss the physical implication of the results. Sec. IV is devoted to the summary of the paper.

## II. FORMALISM

In the calculation of  $g\langle\bar{q}\sigma_{\mu\nu}G_{\mu\nu}q\rangle$  and  $\langle\bar{q}q\rangle$ , we use the  $SU(3)_c$  lattice QCD with the KS fermion at the quenched level. We note that the KS fermion preserves the explicit chiral symmetry for the quark mass  $m=0$ , which is a desirable feature to study both the condensates of chiral order parameters. In order to evaluate the condensates, we calculate the  $SU(4)_f$  flavor-averaged condensates on the lattice as

$$a^3\langle\bar{q}q\rangle = -\frac{1}{4}\sum_f \text{Tr}[\langle q^f(x)\bar{q}^f(x)\rangle] \quad (2)$$

and

$$a^5 g\langle\bar{q}\sigma_{\mu\nu}G_{\mu\nu}q\rangle = -\frac{1}{4}\sum_{f,\mu,\nu} \text{Tr}[\langle q^f(x)\bar{q}^f(x)\rangle\sigma_{\mu\nu}G_{\mu\nu}^{\text{lat}}(x)]. \quad (3)$$

Here, ‘‘Tr’’ refers to the trace over the spinor and the color indices, and  $\langle q^f(y)\bar{q}^f(x)\rangle$  denotes the Euclidean quark propagator of the  $f$ -th flavor. For the gluon field strength  $G_{\mu\nu}^{\text{lat}}$ , we adopt the clover-type definition on the lattice to eliminate  $\mathcal{O}(a)$  discretization error,

$$G_{\mu\nu}^{\text{lat}} = \frac{i}{8}\text{Tr}[\lambda^A(U_{\mu\nu} + U_{\nu-\mu} + U_{-\mu-\nu} + U_{-\nu\mu})] + \text{c.c.}, \quad (4)$$

where  $U_{\mu\nu}$  denotes the plaquette operator, and  $\lambda^A$  ( $A=1,2,\dots,8$ ) is the color  $SU(3)$  Gell-Mann matrix. In the KS-fermion formalism,  $SU(4)_f$  quark-spinor fields,  $q$  and  $\bar{q}$ , are converted into single-component Grassmann KS fields,  $\chi$  and  $\bar{\chi}$ , respectively, with the proper insertion of gauge-link variables which ensure the gauge covariance [12]. Note that

the contraction of flavor and spinor indices corresponds to summation over the KS hypercube [12] and suppresses  $\mathcal{O}(a)$  discretization error. The detailed formulations and the diagrammatic representations for the calculation of the condensates are given in Ref. [12].

We perform Monte Carlo simulations with the standard Wilson gauge action for  $\beta\equiv 2N_c/g^2=6.0, 6.1, \text{ and } 6.2$ . The lattice units are obtained as  $a^{-1}=1.9, 2.3, \text{ and } 2.7$  GeV for  $\beta=6.0, 6.1, \text{ and } 6.2$ , respectively, where we use the lattice data [15] with the string tension  $\sqrt{\sigma}=427$  MeV.

In order to perform the calculation at various temperatures, we use the following lattices,

- (i)  $\beta=6.0$ ,  $V=16^3\times N_t$  ( $N_t=16,12,10,8,6,4$ ),
- (ii)  $\beta=6.1$ ,  $V=20^3\times N_t$  ( $N_t=20,12,10,8,6$ ),
- (iii)  $\beta=6.2$ ,  $V=24^3\times N_t$  ( $N_t=24,16,12,10,8$ ),

which correspond to  $0\leq T\leq 500$  MeV with the spatial volume of  $L^3\approx(1.6-1.8\text{ fm})^3$ . The critical temperature  $T_c$  is obtained from the Polyakov-loop susceptibility [16] in terms of the confinement/deconfinement phase transition. From the Polyakov-loop susceptibility on the above three lattices, we obtain  $T_c/\sqrt{\sigma}\approx 0.64$ , or  $T_c\approx 280$  MeV, which is consistent with Ref. [16].

We generate 100 gauge configurations for each lattice, where we pick up each configuration for every 500 sweeps after 1000 sweeps for the thermalization. In the vicinity of the phase transition point, namely,  $20^3\times 8$  at  $\beta=6.1$  and  $24^3\times 10$  at  $\beta=6.2$ , the fluctuations of the condensates get larger. We hence generate 1000 gauge configurations on these two lattices for the accurate estimate. For the lattices at  $T>T_c$ , we only use the gauge configurations which are continuously connected to the trivial vacuum  $U_\mu=1$ .

To obtain the condensates, we calculate the Euclidean propagator by solving the matrix inverse equations. Here, we use the current-quark mass of  $ma=0.0105, 0.0184$  and  $0.0263$  ( $\beta=6.0$ ),  $ma=0.00945, 0.0162$  and  $0.0234$  ( $\beta=6.1$ ) and  $ma=0.00770, 0.0134$  and  $0.0192$  ( $\beta=6.2$ ), which correspond to the physical mass of  $m\approx 20, 35, \text{ and } 50$  MeV, respectively. For the KS fields,  $\chi$  and  $\bar{\chi}$ , the antiperiodic condition is imposed at the boundary in both the temporal and spatial directions. In each configuration, we measure the condensates on 16 different physical space-time points at  $\beta=6.0$  and 2 points at  $\beta=6.1$  and  $6.2$ . These points are taken so as to be equally spaced in the lattice 4-dimensional volume, i.e., on the lattices with the volume  $V=L^3\times N_t\equiv(2l)^3\times(2n_t)$  in the lattice unit, we take 16 points at  $\beta=6.0$  as  $x=(x_1,x_2,x_3,x_4)$  with  $x_i\in\{0,l\}$  ( $i=1,2,3$ ),  $x_4\in\{0,n_t\}$ , and 2 points at  $\beta=6.1$  and  $6.2$  as  $x\in\{(0,0,0),(l,l,l,n_t)\}$ . In addition, the summation over the KS hypercube is taken on each selected space-time point. At each quark mass  $m$  and temperature, we thus achieve high statistics as 1600 data at  $\beta=6.0$  and 200 data at  $\beta=6.1$  and  $6.2$ . Note that for the lattices of  $20^3\times 8$  ( $\beta=6.1$ ) and  $24^3\times 10$  ( $\beta=6.2$ ), we obtain 2000 data, which guarantees reliability of the results even in the vicinity of the critical temperature.

At each temperature, we calculate the condensates  $\langle\bar{q}q\rangle$  and  $g\langle\bar{q}\sigma_{\mu\nu}G_{\mu\nu}q\rangle$  at three different quark masses,  $m$ . We observe that both the condensates show a clear linear behav-

ior against the quark mass at every finite temperature, as was seen in Ref. [12] at  $T=0$ . Therefore, we fit the data with a linear function and determine the condensates in the chiral limit.

We comment here on the error estimate and the numerical check on the finite-volume effect in lattice QCD. The statistical error is estimated with the jack-knife method. In the vicinity of  $T_c$ , i.e., on  $20^3 \times 8$  at  $\beta=6.1$  and  $24^3 \times 10$  at  $\beta=6.2$ , we conservatively suppress the autocorrelation by performing binning of the size of 10. We find that the statistical error is typically 5–7% level for every temperature. For the check of the finite-volume artifact, we examine the condensates imposing the periodic condition on the KS fields,  $\chi$  and  $\bar{\chi}$ , instead of the antiperiodic condition, at the 3-dimensional spatial boundaries. We perform the calculations with typical lattices of  $24^3 \times 10$  ( $\beta=6.2$ ) and  $16^3 \times 4$  ( $\beta=6.0$ ), which corresponds to  $T \approx T_c$  and  $T_c \ll T$ , respectively, and find that the dependence of the condensates on the spatial boundary condition is only 1% level. For  $T \ll T_c$  lattice case, it was shown that the finite-volume artifact for  $16^4$  ( $\beta=6.0$ ) lattice is only 1% level in Ref. [12]. We therefore conclude that the physical volume  $L^3 \approx (1.6 \text{ fm})^3$  in our simulations is large enough to avoid the finite volume artifact.

### III. THE LATTICE QCD RESULTS AND DISCUSSIONS

We estimate the thermal effects on each condensate,  $g\langle\bar{q}\sigma_{\mu\nu}G_{\mu\nu}q\rangle$ , or  $\langle\bar{q}q\rangle$ , by taking the ratio between the values at finite and zero temperatures. In this ratio, the renormalization constants are canceled because there is no operator mixing for both the condensates in the chiral limit [17]. Here, at each  $\beta$ , we use the value at the lowest temperature as a substitute for the value at zero temperature. This approximation can be justified because the finite-volume artifact for the lowest temperature is almost negligible, as was shown for  $16^4$  ( $\beta=6.0$ ) lattice.

In Fig. 1, we plot the thermal effects on  $g\langle\bar{q}\sigma_{\mu\nu}G_{\mu\nu}q\rangle$ . We find a drastic change of  $g\langle\bar{q}\sigma_{\mu\nu}G_{\mu\nu}q\rangle$  around the critical temperature  $T_c \approx 280$  MeV. This is the first observation of chiral-symmetry restoration through  $g\langle\bar{q}\sigma_{\mu\nu}G_{\mu\nu}q\rangle$ . We obtain  $T_c/\sqrt{\sigma}=0.64(4)$ , which is consistent with the coincidence of the confinement/deconfinement phase transition and chiral-symmetry phase restoration. We also find that the thermal effects on  $g\langle\bar{q}\sigma_{\mu\nu}G_{\mu\nu}q\rangle$  are remarkably weak below  $T_c$ , namely,  $T \leq 0.9T_c$ . In Fig. 2, the thermal effects on  $\langle\bar{q}q\rangle$  are plotted, and the same features as  $g\langle\bar{q}\sigma_{\mu\nu}G_{\mu\nu}q\rangle$  are obtained.

We then quantitatively compare the thermal effects of  $g\langle\bar{q}\sigma_{\mu\nu}G_{\mu\nu}q\rangle$  and  $\langle\bar{q}q\rangle$ . For this purpose, we plot the ratio  $m_0^2(T) \equiv g\langle\bar{q}\sigma_{\mu\nu}G_{\mu\nu}q\rangle_T / \langle\bar{q}q\rangle_T$  normalized by  $m_0^2(T=0)$  for  $T \leq T_c$  in Fig. 3. We observe that  $m_0^2(T)$  is almost independent of the temperature, even in the very vicinity of  $T_c$ , which can be interpreted to mean that  $g\langle\bar{q}\sigma_{\mu\nu}G_{\mu\nu}q\rangle_T$  and  $\langle\bar{q}q\rangle_T$  obey the same thermal behavior. This result is rather nontrivial because, as was noted before, these two condensates characterize different aspects of the QCD vacuum.

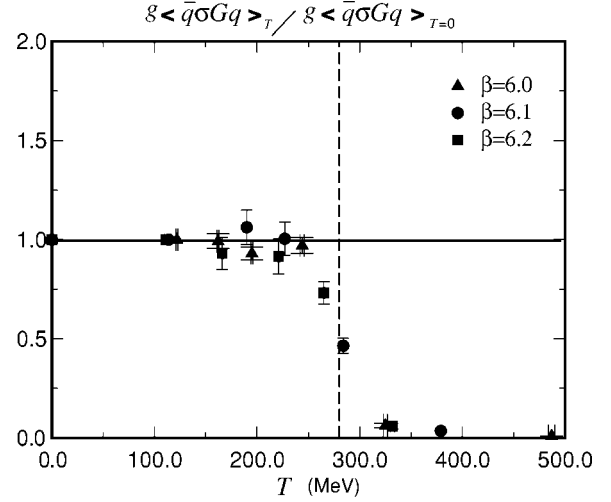


FIG. 1. The quark-gluon mixed condensate  $g\langle\bar{q}\sigma_{\mu\nu}G_{\mu\nu}q\rangle_T$  at finite temperature  $T$  normalized by  $g\langle\bar{q}\sigma_{\mu\nu}G_{\mu\nu}q\rangle_{T=0}$ . The vertical dashed line denotes the critical temperature  $T_c \approx 280$  MeV in quenched QCD.

As a new interesting feature absent in the scalar-type condensate  $\langle\bar{q}q\rangle$ ,  $g\langle\bar{q}\sigma_{\mu\nu}G_{\mu\nu}q\rangle$  may reveal possible breaking of the space-time duality in Euclidean QCD at finite temperature. For further analysis in this direction, we investigate the thermal effects on electric/magnetic components of  $g\langle\bar{q}\sigma_{\mu\nu}G_{\mu\nu}q\rangle$  separately, i.e.,  $g\langle\bar{q}\sigma_{4i}G_{4i}q\rangle$  and  $g\langle\bar{q}\sigma_{jk}G_{jk}q\rangle$ . Hereafter, no summation is taken for  $i, j, k \in \{1, 2, 3\}$ . Of course, the equality  $g\langle\bar{q}\sigma_{4i}G_{4i}q\rangle = g\langle\bar{q}\sigma_{jk}G_{jk}q\rangle$  holds at zero temperature from O(4) symmetry in Euclidean QCD. This equality, however, does not necessarily hold for finite temperature, where the space-time duality is explicitly broken. In fact, at finite temperature,  $g\langle\bar{q}\sigma_{4i}G_{4i}q\rangle_T$  and  $g\langle\bar{q}\sigma_{jk}G_{jk}q\rangle_T$  can be regarded as different chiral order parameters.

We therefore plot the ratio  $R_{E/B}(T)$  defined by

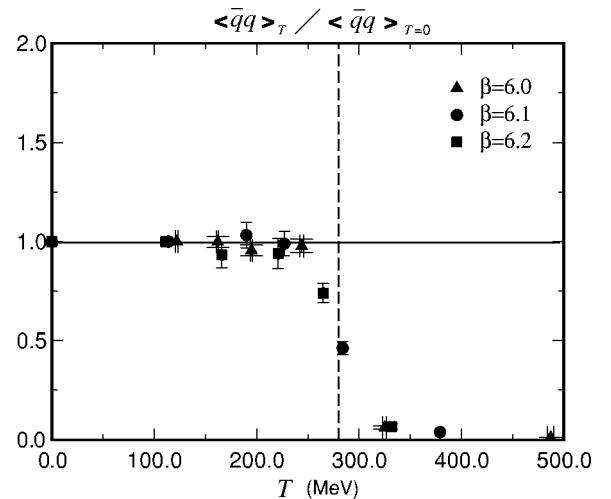


FIG. 2. The quark condensate  $\langle\bar{q}q\rangle_T$  at finite temperature  $T$  normalized by  $\langle\bar{q}q\rangle_{T=0}$ . The vertical dashed line denotes  $T_c$ .

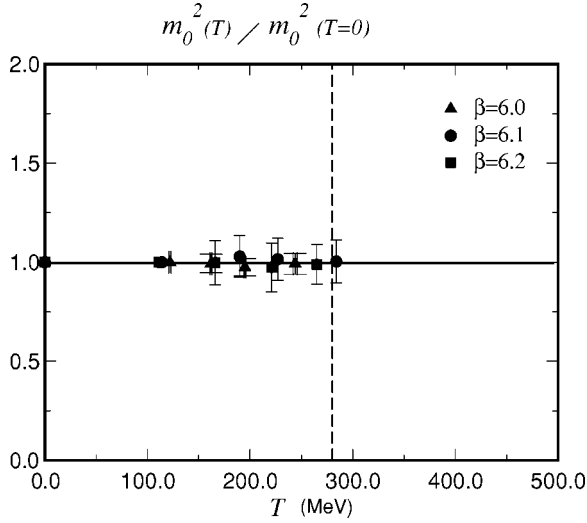


FIG. 3. The ratio  $m_0^2(T) \equiv g\langle\bar{q}\sigma_{\mu\nu}G_{\mu\nu}q\rangle_T / \langle\bar{q}q\rangle_T$  normalized by  $m_0^2(T=0)$  plotted against  $T$ . This result indicates the same chiral behavior between  $g\langle\bar{q}\sigma_{\mu\nu}G_{\mu\nu}q\rangle_T$  and  $\langle\bar{q}q\rangle_T$ .

$$R_{E/B}(T) \equiv \frac{\sum_i g\langle\bar{q}\sigma_{4i}G_{4i}q\rangle_T}{\sum_{j<k} g\langle\bar{q}\sigma_{jk}G_{jk}q\rangle_T} \quad (5)$$

at finite temperature  $T \lesssim T_c$  in Fig. 4. One sees that the equality  $g\langle\bar{q}\sigma_{4i}G_{4i}q\rangle_T = g\langle\bar{q}\sigma_{jk}G_{jk}q\rangle_T$  holds for even at finite temperature. This again indicates that all the  $(\mu, \nu)$  components of  $g\langle\bar{q}\sigma_{\mu\nu}G_{\mu\nu}q\rangle_T$  obey the same chiral behavior near  $T_c$ .

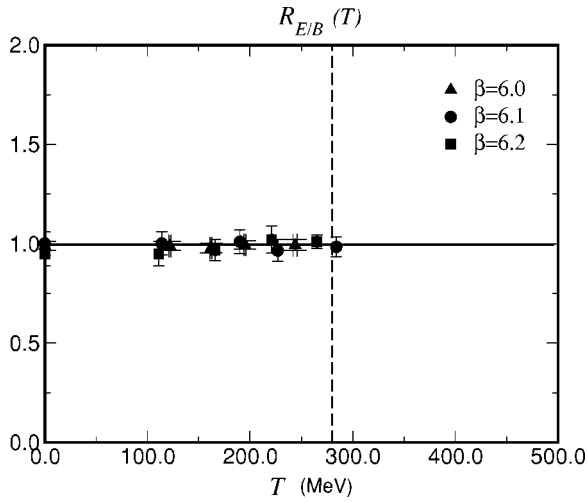


FIG. 4. The ratio  $R_{E/B}(T) \equiv \sum_i g\langle\bar{q}\sigma_{4i}G_{4i}q\rangle_T / \sum_{j<k} g\langle\bar{q}\sigma_{jk}G_{jk}q\rangle_T$  plotted against the temperature  $T$ . This result indicates  $g\langle\bar{q}\sigma_{4i}G_{4i}q\rangle_T$  and  $g\langle\bar{q}\sigma_{jk}G_{jk}q\rangle_T$  obey the same chiral behavior.

In this way, we observe that the chiral condensates, i.e.,  $\langle\bar{q}q\rangle_T$ ,  $g\langle\bar{q}\sigma_{\mu\nu}G_{\mu\nu}q\rangle_T$ ,  $g\langle\bar{q}\sigma_{4i}G_{4i}q\rangle_T$ , and  $g\langle\bar{q}\sigma_{jk}G_{jk}q\rangle_T$ , obey the almost identical behavior near  $T_c$ . One of the possible explanations of this similarity is given by the so-called ‘‘Swiss cheese picture.’’ In this picture, phase structure of the QCD vacuum at the critical temperature is represented by the mixture of coexisting two phases, i.e., chiral-broken phase and chiral-symmetric phase. Since the deconfinement phase transition is of the first order in the quenched approximation, the coexistence of two phases is plausible. In this scenario, the common thermal behaviors of the chiral condensates can be explained if the thermal effects are mainly characterized by the volume ratio of the two phases and the thermal effects on each phase are subdominant. Since this consideration can be applied to any chiral condensates, this scenario predicts a universal behavior of all chiral order parameters near  $T_c$ , which provides new aspects on the chiral structure of the QCD phase transition.

The common thermal behaviors of the chiral condensates can be also explained from a different viewpoint. Following Refs. [18,19], we can express the condensates as

$$\langle\bar{q}q\rangle = \frac{1}{V} \int d\lambda' \frac{m\rho(\lambda')}{\lambda'^2 + m^2},$$

$$g\langle\bar{q}\sigma_{\mu\nu}G_{\mu\nu}q\rangle = \frac{1}{V} \int d\lambda' \frac{m\rho(\lambda')}{\lambda'^2 + m^2} \langle\lambda'|\sigma_{\mu\nu}G_{\mu\nu}|\lambda'\rangle, \quad (6)$$

where  $|\lambda\rangle$  denotes the eigenvector of the Dirac operator as  $i\mathcal{D}|\lambda\rangle = \lambda|\lambda\rangle$ , and  $\rho(\lambda)$  the spectral density on  $\lambda$ . When one takes the chiral limit  $m \rightarrow 0$  after the thermodynamic limit  $V \rightarrow 0$ , the zero modes ( $\lambda = 0$ ) of the Dirac operator are responsible for both the condensates. If  $\langle\lambda|\sigma_{\mu\nu}G_{\mu\nu}|\lambda\rangle$  does not have a singularity at  $\lambda = 0$ ,  $m_0^2$  corresponds to  $\langle\lambda|\sigma_{\mu\nu}G_{\mu\nu}|\lambda\rangle|_{\lambda=0}$ . The universal chiral behavior against the temperature indicates that both the electric and the magnetic components of  $\langle\lambda|\sigma_{\mu\nu}G_{\mu\nu}|\lambda\rangle|_{\lambda=0}$  for the chiral zero modes have remarkably weak dependence on the temperature for  $T \lesssim T_c$ , even in the very vicinity of  $T_c$ .

#### IV. SUMMARY

We have studied thermal effects on  $g\langle\bar{q}\sigma_{\mu\nu}G_{\mu\nu}q\rangle$ , in comparison with  $\langle\bar{q}q\rangle$ , using the  $SU(3)_c$  lattice QCD with the KS fermion at the quenched level. For  $T \lesssim 0.9T_c$ , both the condensates show very little thermal effect, while a clear signal of chiral restoration is observed near  $T_c$  as a sharp decrease of both the condensates. It has been a surprise that the ratio  $m_0^2(T) \equiv g\langle\bar{q}\sigma_{\mu\nu}G_{\mu\nu}q\rangle_T / \langle\bar{q}q\rangle_T$ , in contrast to the drastic change of each, is almost independent of the temperature in the entire region of  $T$  up to  $T_c$ . It is also found that the Lorentz components,  $g\langle\bar{q}\sigma_{4i}G_{4i}q\rangle_T$  and  $g\langle\bar{q}\sigma_{jk}G_{jk}q\rangle_T$ ,

show an identical temperature dependence. Such observations indicate that these chiral condensates show a common thermal behavior, which may reveal new aspects of the chiral restoration of the QCD vacuum. For further studies, a full QCD lattice calculation is in progress in order to analyze the dynamical quark effects on the condensates. Through the full QCD calculation and its comparison with quenched QCD, we expect to get deeper insight on the chiral structure of the QCD vacuum at finite temperature.

## ACKNOWLEDGMENTS

This work is supported in part by the Grant for Scientific Research [(B) No. 15340072 and No. 13011533] from the Ministry of Education, Culture, Science and Technology, Japan. T.D. acknowledges the support by the Japan Society for the Promotion of Science for Young Scientists. The Monte Carlo simulations have been performed on the NEC SX-5 supercomputer at Osaka University and IBM POWER4 Regatta system at Tokyo Institute of Technology.

- 
- [1] G.K. Savvidy, Phys. Lett. **71B**, 133 (1977); N.K. Nielsen and P. Olesen, Nucl. Phys. **B144**, 376 (1978).
  - [2] S. Narison, *QCD Spectral Sum Rules* (World Scientific, Singapore, 1989), p. 1 and references therein.
  - [3] B.L. Ioffe, Nucl. Phys. **B188**, 317 (1981); **B191**, 591 (1981).
  - [4] H.G. Dosch, M. Jamin, and S. Narison, Phys. Lett. B **220**, 251 (1989); W.-Y.P. Hwang and K.-C. Yang, Phys. Rev. D **49**, 460 (1994).
  - [5] D. Jido, N. Kodama, and M. Oka, Phys. Rev. D **54**, 4532 (1996); D. Jido and M. Oka, hep-ph/9611322.
  - [6] J. Sugiyama, T. Doi, and M. Oka, Phys. Lett. B **581**, 167 (2004).
  - [7] T. Nakano *et al.*, Phys. Rev. Lett. **91**, 012002 (2003).
  - [8] H.G. Dosch and S. Narison, Phys. Lett. B **417**, 173 (1998) and references therein.
  - [9] J.I. Latorre, P. Pascual, and S. Narison, Z. Phys. C **34**, 347 (1987).
  - [10] V.M. Belyaev and B.L. Ioffe, Zh. Éksp. Teor. Fiz. **83**, 876 (1982) [Sov. Phys. JETP **56**, 493 (1982)].
  - [11] M. Kremer and G. Schierholz, Phys. Lett. B **194**, 283 (1987).
  - [12] T. Doi, N. Ishii, M. Oka, and H. Suganuma, Phys. Rev. D **67**, 054504 (2003).
  - [13] T.W. Chiu and T.H. Hsieh, Nucl. Phys. **B673**, 217 (2003).
  - [14] T. Doi, N. Ishii, M. Oka, and H. Suganuma, Nucl. Phys. **A721**, 934 (2003); Prog. Theor. Phys. Suppl. **151**, 161 (2003); Nucl. Phys. B (Proc. Suppl.) **129**, 566 (2004); T. Doi, H. Suganuma, M. Oka, and N. Ishii, in *Color Confinement and Hadrons in Quantum Chromodynamics (Confinement 2003)* (World Scientific, Singapore, 2004), p. 398.
  - [15] M. Gockeler, R. Horsley, H. Perlt, P. Rakow, G. Schierholz, A. Schiller, and P. Stephenson, Phys. Rev. D **57**, 5562 (1998).
  - [16] G. Boyd, J. Engels, F. Karsch, E. Laermann, C. Legeland, M. Lutgemeier, and B. Petersson, Nucl. Phys. **B469**, 419 (1996); N. Ishii, H. Suganuma, and H. Matsufuru, Phys. Rev. D **66**, 094506 (2002).
  - [17] S. Narison and R. Tarrach, Phys. Lett. **125B**, 217 (1983).
  - [18] T. Banks and A. Casher, Nucl. Phys. **B169**, 103 (1980).
  - [19] S. Hands, J.B. Kogut, and A. Kocic, Nucl. Phys. **B357**, 467 (1991).